Supplementary Information

Design and Integration of Glass-fiber-cloth Networks in PEO-LLZTO Composite: A Multifunctional Approach for Electrolyte Engineering

Fu-Wei Chang, Che-Ya Wua, Tzu-Ying Lin*

Department of Materials Science and Engineering, National Tsing Hua University, Hsinchu, Taiwan

*Corresponding author E-mail: tzuying.lin@mx.nthu.edu.tw

1. Experimental Section

Poly(ethylene oxide) (PEO, Mw = 600,000, Acros Organics) and lithium bis(trifluoromethanesulfonyl)imide (LiTFSI, 98+%, ALFA) were dried under vacuum at 60°C for 24 h and stored in an Ar-filled glove box. The polymer electrolyte was prepared by dissolving PEO (0.5 g) and LiTFSI (0.3262 g) (corresponding to an [EO]:[Li+] molar ratio of 10:1) in a mixed solvent of N,N-dimethylacetamide (DMAc, 98+%, ACROS Organics) and acetone (99.8%, ACROS Organics) (volume ratio 1:2, total volume 10 mL). The solution was magnetically stirred at 50°C for 24 h and subsequently cast onto a polytetrafluoroethylene (PTFE) mold. After solvent evaporation, the resulting film was dried at 60°C for 24 h, followed by vacuum drying at the same temperature for an additional 24 h.

To fabricate the composite polymer electrolytes (CPEs), $Li_{6.4}La_3Zr_{1.4}Ta_{0.6}O_{12}$ (LLZTO, particle diameter: 5-8 μm, China Glaze) and glass fiber cloth (GFC, thickness: 30 μm, PENG SHENG CO., LTD.) were incorporated into the solid polymer electrolyte. The preparation procedure was modified as follows: LLZTO powder was added to the homogeneous PEO-LiTFSI solution and magnetically stirred at 50°C for 24 h. The resulting suspension was then used to impregnate the GFC. The composite was dried at 60°C for 24 h, followed by vacuum drying at 60°C for an additional 24 h. Following this procedure, three types of electrolytes were prepared for comparative studies: PEO-LiTFSI, PEO-LiTFSI@GFC, and PEO-LiTFSI-LLZTO@GFC.

2. Electrochemical Test and Characterization

Ionic conductivity, linear sweep voltammetry (LSV) and Li^+ number (t_{Li}^+) were characterized with a PARSTAT 2273 (Princeton Applied Research) electrochemical workstation. All the battery was assembled with CR203 coin cells.

For ionic conductivity measurement, the CPEs were sandwiched between two 15.5 mm stainless steel (SS) sheets. Electrochemical impedance spectroscopy (EIS) testing was conducted from room temperature to 70 ºC in the frequency range of 10^{-1}~2×10^6 Hz with an amplitude of 70 mV. The ionic conductivity (σ) was calculated by the following formula.

$$\sigma = \frac{L}{RA} \qquad (1)$$

where L is the thickness of the polymer electrolyte membrane, R is the impedance, and A is the area of the SS. The activation energy (E_a) was calculated using the Arrhenius equation.

$$\sigma = \mathrm{A}\exp\left(-\frac{E_a}{RT}\right) \qquad (2)$$

where σ is ionic conductivity, A is the frequency factor, R is the gas molar constant, and T is the absolute temperature.

Linear scanning voltammetry (LSV) test was conducted on a Li| CPEs |SS coin cell to obtain the electrochemical stability window of the CPEs. The scanning rate was 5 mV s^{-1} and the scanning voltage started from open circuit to 3.5V relative to the open circuit.

The lithium-ion transference number (t_{Li}^{+}) was determined using chronoamperometry and calculated based on the following equation.

$$\text{Bruce-Vincent equation:} \qquad t_{Li+} = \frac{I_{ss}(\Delta V - I_0 R_0)}{I_0(\Delta V - I_{ss} R_{ss})} \qquad (3)$$

where I_0 is the initial current, I_{ss} is the steady-state current, R_0 is the interfacial resistance before polarization, R_{ss} is the interfacial resistance after polarization, and ΔV is the applied voltage bias (10 mV).

To evaluate the electrochemical performance of the CPE, the $LiFePO_4$ (LFP)||Li battery was assembled. the LFP cathode contains 80 wt.% LFP, 9 wt.% carbon black, 1wt.% CNT, and 10wt.%PVDF. The batteries were assembled using a CR2032 coin cell in a glove box (H_2O < 0.1 ppm, O_2 < 5 ppm) filled with argon. During assembling, 10 μL of liquid electrolyte was added. Arbin charge-discharge instrument (BT2000, Arbin instrument) was applied to determine the cycling performance. Electrochemical impedance spectra (EIS) were measured at the frequency range from 2 MHz to 0.1 Hz with an AC voltage of 70 mV.

The morphology and microstructure of the material were observed by field emission scanning electron microscopy (FESEM,JSM-IT800, JEOL). The phase structure of the material was examined by X-ray diffraction (XRD, D2 PHASER, Bruker) with Cu Ka radiation source (λ = 1.5415 Å). Fourier Transform Infrared Spectroscopy (FTIR, FT/IR-4600, JASCO) and Raman spectroscopy (Raman, WITec Alpha 300R, WITec) were used to investigate the chemical environment of the CPEs. Thermal stabilities were tested using a Thermogravimetric analyzer (TGA, Mettler-Toledo, 2-HT). The test was performed from 25 ºC to 800 ºC at a heating rate of 10 ºC/min in an air atmosphere.

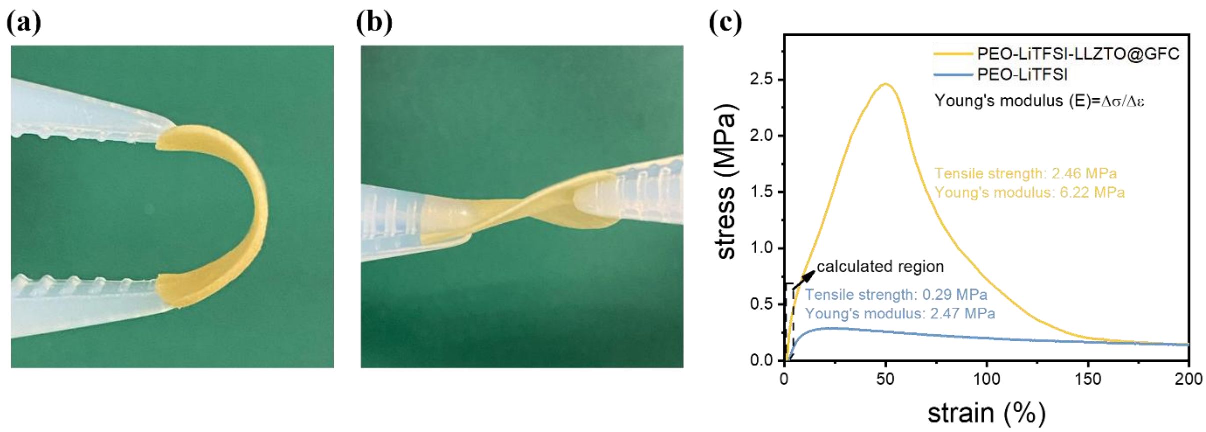

Fig. S1 Optical photographs of (a) bending and (b) twisting test of PEO-LiTFSI-LLZTO@GFC at 25 ºC. (c) Stress-strain curves of PEO-LiTFSI, and PEO-LiTFSI-LLZTO@GFC. Young’s modulus (calculated from the slope of the initial linear region of the stress-strain curves) improves from 2.47 MPa to 6.22 MPa.

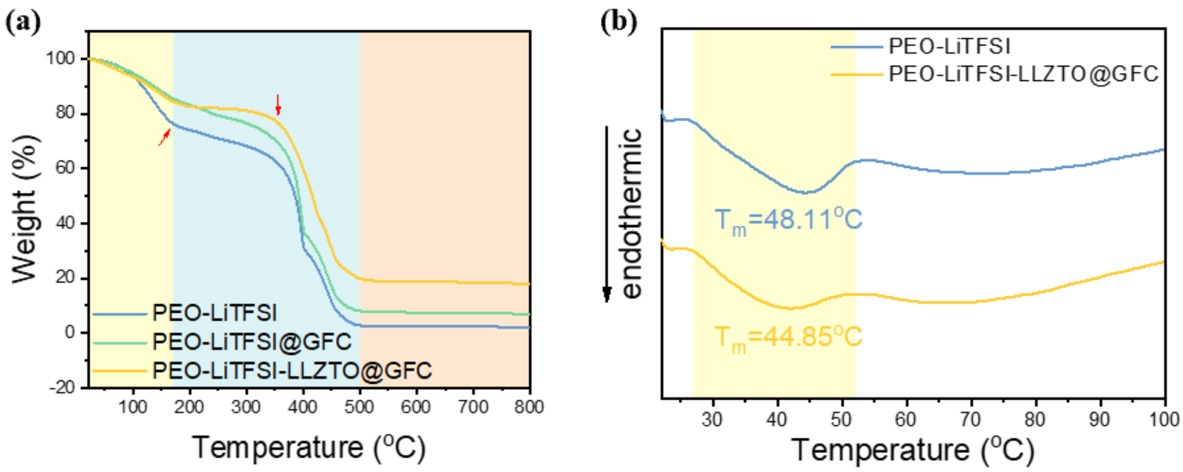

Fig. S2 (a) Thermogravimetric analysis (TGA) curve of PEO-LiTFSI (blue line), PEO-LiTFSI@GFC (green line), and PEO-LiTFSI-LLZTO@GFC (yellow line). The red arrows indicate the deformation temperature of PEO-LiTFSI and PEO-LiTFSI-LLZTO@GFC, respectively. (b) Differential scanning calorimetry (DSC) curves of PEO-LiTFSI and PEO-LiTFSI-LLZTO@GFC CPEs. DSC experiment was conducted under nitrogen atmosphere.

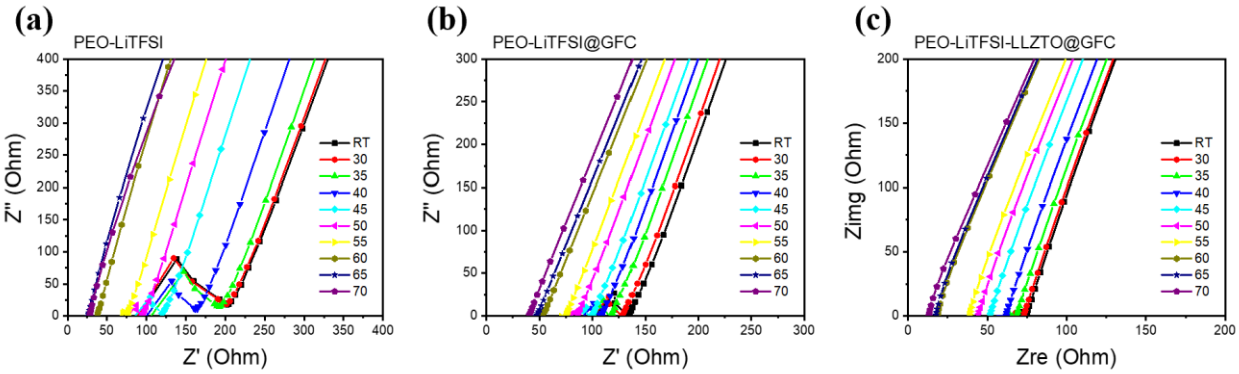

Fig. S3 Nyquist plots of stainless-steel symmetric cells under various temperature using (a) PEO-LiTFSI (b) PEO-LiTFSI@GFC (c) PEO-LiTFSI-LLZTO@GFC electrolytes.

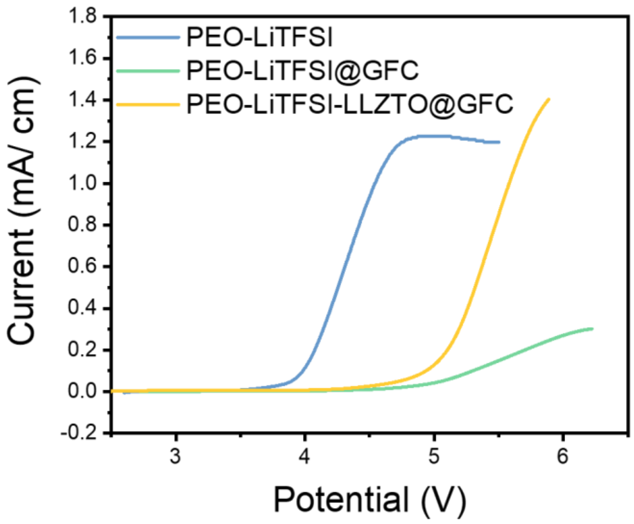

Fig. S4 Linear sweep voltammetry (LSV) curves of the PEO-LiTFSI, PEO-LiTFSI@GFC, and PEO-LiTFSI-LLZTO@GFC.

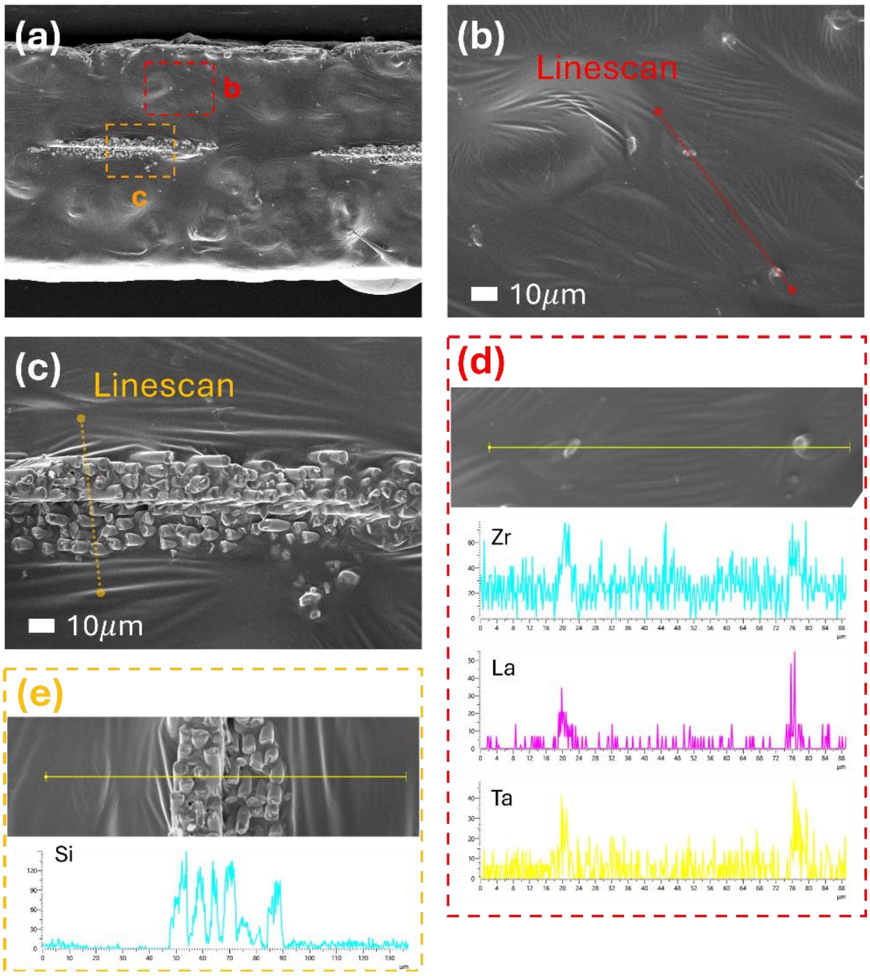

Fig. S5 Cross-sectional FESEM images and corresponding EDS line scans of the PEO-LiTFSI-LLZTO@GFC membrane: (a) overall cross-section, (b) lateral region, and (c) central region containing embedded glass-fiber-cloth. (d) EDS line scan of the lateral region confirming the presence of LLZTO ceramic fillers (Zr, La, Ta signals), and (e) EDS line scan of the central region confirming the presence of glass fiber cloth (Si signal).

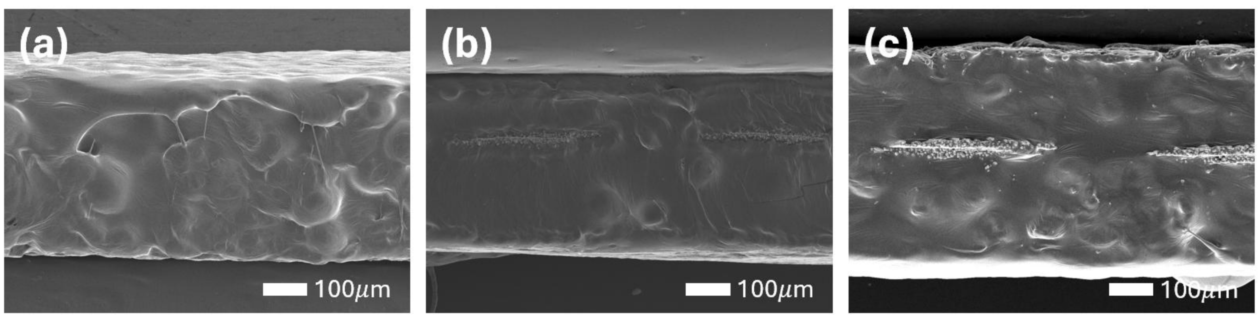

Fig. S6 Cross-sectional SEM images of (a) PEO-LiTFSI, (b) PEO-LiTFSI@GFC, (c) PEO-LiTFSI-LLZTO@GFC.

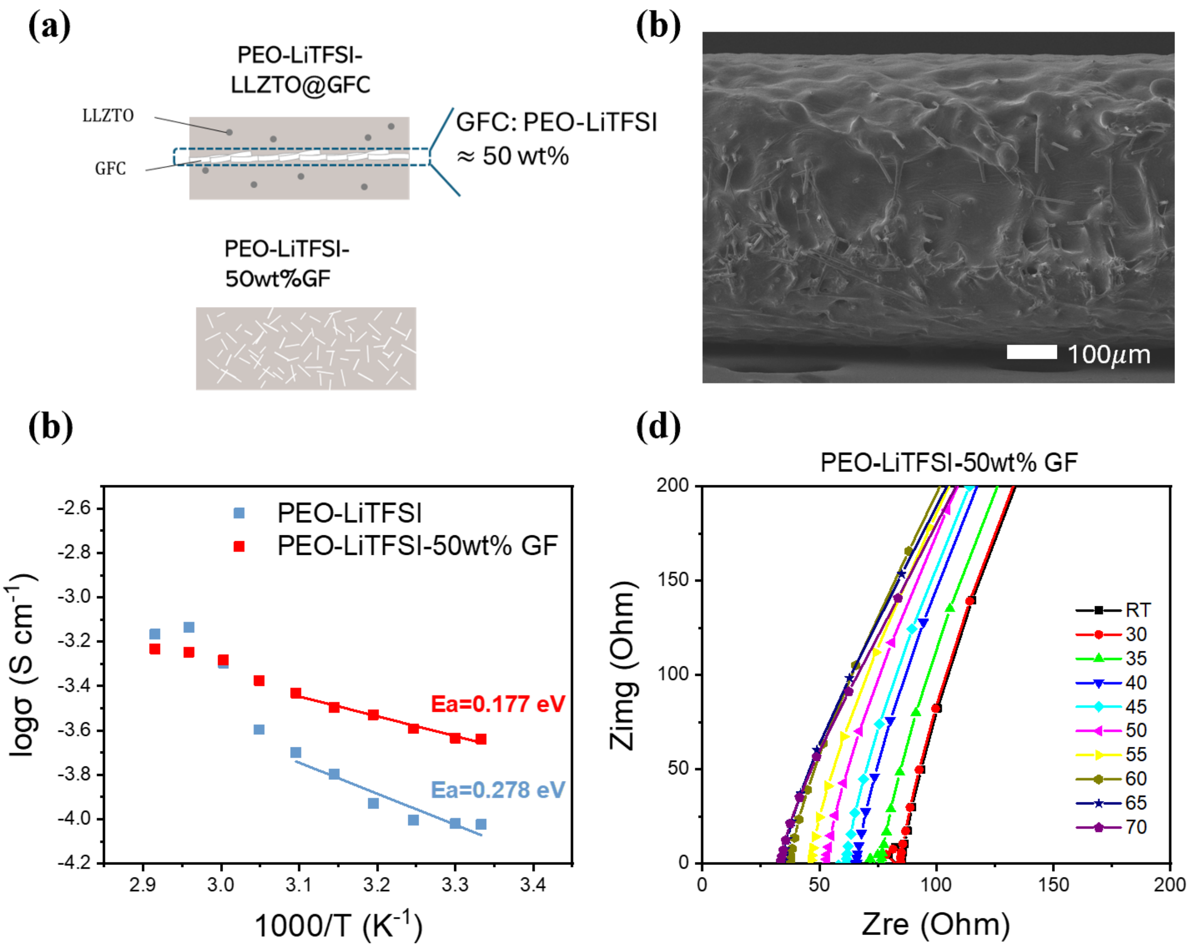

Fig. S7 (a) The schematic diagram illustrates the design of a new electrolyte system aimed at verifying the role of the central layer in enhancing Li+ concentration. This system incorporates dispersed glass fibers with a GFC: PEO-LiTFSI weight ratio of approximately 50 wt% (referred to PEO-LiTFSI-50wt%GF), similar to that of the central layer of PEO-LiTFSI-LLZTO@GFC. Note: The weight ratio of glass fiber in the PEO-LiTFSI-LLZTO@GFC electrolyte was estimated by comparing the mass of glass fiber with that of the PEO electrolyte in the middle 30 μm region. The calculation indicates approximately 50 wt% glass fiber content, with the actual composite structure distributed across a ~45 μm central region in the final membrane. (b) The cross-sectional SEM image. (c) The Arrhenius plot of PEO-LiTFSI-50wt%GF and PEO-LiTFSI electrolytes. (d) Nyquist plots of stainless-steel symmetric cells under various temperature (27 to 70 °C).

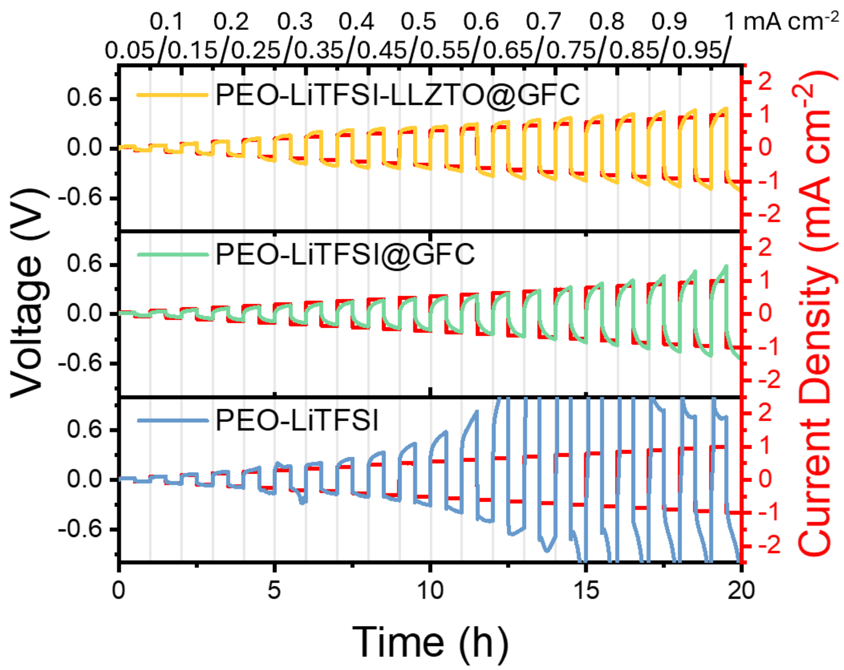

Fig. S8 Voltage profiles of Li||Li symmetric cells at various current densities (0.05-1 mA/cm²) for different electrolyte systems: PEO-LiTFSI-LLZTO@GFC (yellow), PEO-LiTFSI@GFC (green), and PEO-LiTFSI (blue).

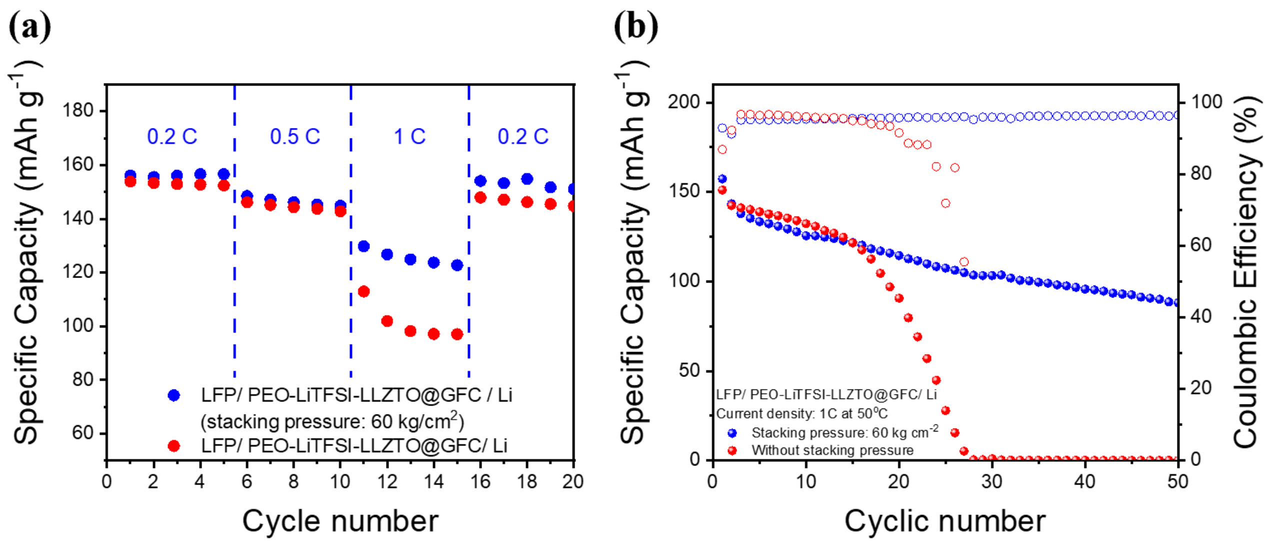

Fig. S9 (a) Rate performance (discharge capacities) of LFP|PEO-LiTFSI-LLZTO@GFC|Li cells. The blue and red circles represent full cell cycling with and without 60 kg/cm^2 stacking pressure, respectively. (b) Cycle performance of LFP|PEO-LiTFSI-LLZTO@GFC|Li cells with and without 60 kg /cm^2 stacking pressure at 1C and 50 °C.

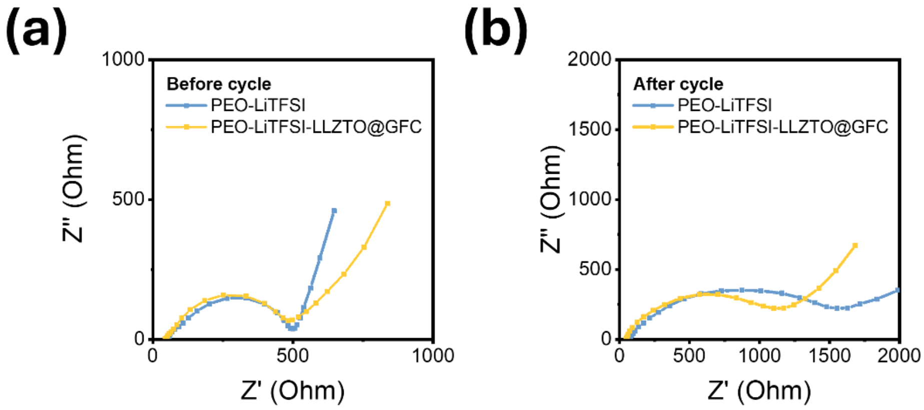

Fig. S10 Nyquist plots of LFP||Li cells with PEO-LiTFSI and PEO-LiTFSI-LLZTO@GFC electrolytes (a) before and (b) after 50 hours cycling at 0.2C and 50 ºC.

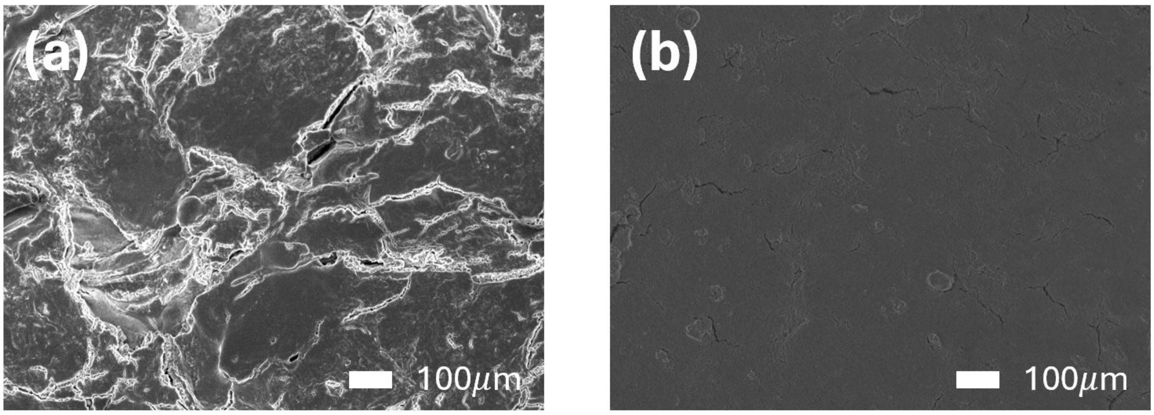

Fig. S11 Surface morphology of Li anodes from (a) LFP|PEO-LiTFSI|Li and (b) LFP|PEO-LiTFSI-LLZTO@GFC|Li cells after 350 hours cycling at 0.2C and 50 ºC.

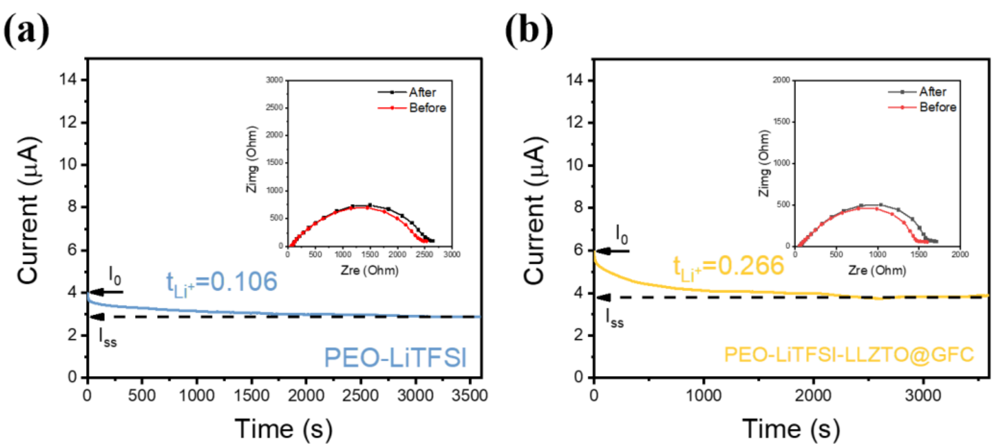

Fig. S12 DC polarization curves of (a) PEO-LiTFSI and (b) PEO-LiTFSI-LLZTO@GFC. Insets: AC impedance spectra before and after polarization.

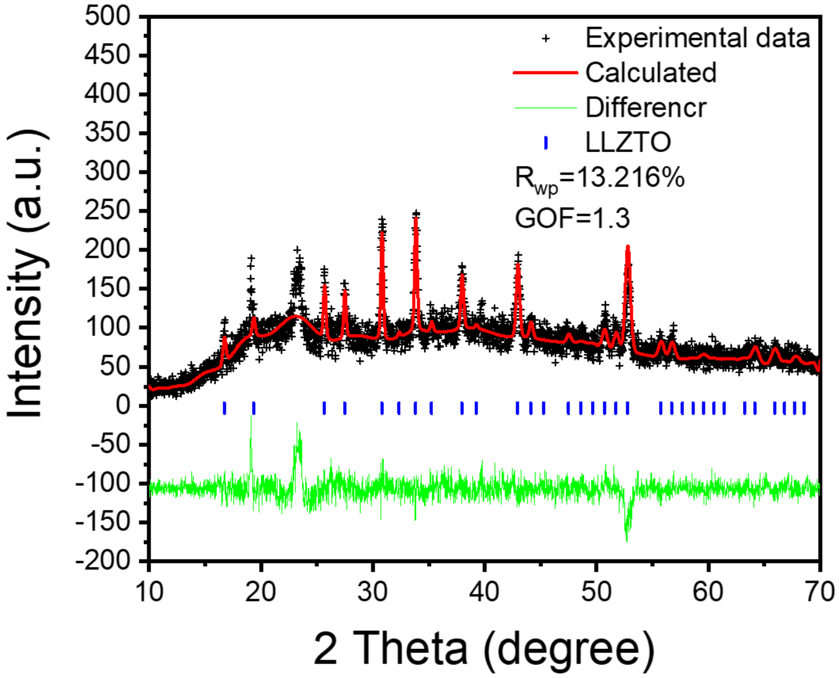

Fig. S13 Rietveld refinement of PEO-LiTFSI-LLZTO@GFC. The GOF (goodness of fit) is 1.3, while R_{wp} (Weighted Profile R-factor) is slightly above 10% (R_{wp} ~13%), primarily due to residual crystalline PEO peaks at 2θ = 19° and 23.15°.

Table S1 Ionic conductivity at different temperature, caculated activation energy in the temperature range of 27°C~50°C and 25°C~70°C, and the corresponding R square (R^2). R^2 is the coefficient of determination, which measures how well the data points fit a linear regression model. An R^2 value of 1 indicates that all data points perfectly align with the fitted line, meaning there is no deviation from linearity.

Electrolytes	Ionic conductivity (S cm^{-1})						E_a (calculated from 25°C to 50°C)
	27°C	30°C	35°C	40°C	45°C	50°C	
PEO-LiTFSI	9.47E-05	9.57E-05	9.92E-05	1.18E-04	1.60E-04	2.00E-04	0.278
PEO-LiTFSI@GFC	1.50E-04	1.57E-04	1.71E-04	1.85E-04	2.00E-04	2.34E-04	0.152
PEO-LiTFSI-LLZTO@GFC	3.00E-04	3.09E-04	3.26E-04	3.63E-04	4.33E-04	4.90E-04	0.181

Table S2 Raw data of Niquist plots at 27°C~50°C. The effect of CPE thickness on the measured values was excluded. The unit of Z (Z' and Z'') is Ohm.

Temp.	27°C		30°C		35°C		40°C		45°C		50°C	
Freq. (Hz)	Z'	Z''	Z'	Z''	Z'	Z''	Z'	Z''	Z'	Z''	Z'	Z''
PEO-LiTFSI												
0.1	199434.8	352228.32	197875.45	345016.1	200569.84	340635.47	195206.97	320033.45	183695.79	280752.62	168810.5	249935.49
0.17854992	123479.68	239816.88	122759	236645.82	127159.55	235348.34	124039.12	222340.73	117006.14	198760.1	110092.27	178546.04
0.31880073	76314.825	160998.72	77267.245	159595.1	79191.663	160036.81	77714.379	151416.03	73679.447	137064.78	69827.197	124507.33
0.56921845	47071.95	106777.61	48640.189	105632.94	49035.275	106709.71	48575.539	102012.54	46216.788	92963.271	43430.251	84965.644
1.0163391	29500.635	70295.645	30005.18	69981.423	30930.627	70781.609	30612.796	68048.459	29089.332	62559.798	27341.203	57731.614
1.8146726	18287.118	45719.592	18711.07	45594.004	19145.443	46292.72	18953.279	44772.296	17974.253	41403.389	16900.324	38364.649
3.2400964	11427.58	29613.222	11712.031	29643.531	11953.694	30160.775	11788.556	29266.239	11104.463	27191.299	10359.698	25264.911
5.7851894	7109.8523	19024.228	7288.7902	19107.655	7402.2603	19457.325	7264.623	18925.321	6770.5915	17628.155	6280.1084	16397.78
10.329451	4494.9032	12173.041	4604.0531	12260.457	4646.5554	12483.684	4537.5316	12163.328	4181.987	11334.792	3846.9169	10540.899
18.443226	2832.8816	7743.8157	2896.7984	7821.0728	2903.6528	7956.2471	2822.1581	7762.134	2566.028	7226.3794	2341.7301	6713.802
32.930365	1779.1338	4825.221	1812.5648	4883.3066	1803.2033	4963.3065	1736.8588	4844.8338	1556.2485	4505.4296	1407.5008	4180.5201
58.79714	1182.3939	3107.72	1199.7278	3150.2269	1183.9162	3197.1604	1127.288	3121.6395	993.02256	2897.2939	889.04289	2684.3655
104.98225	794.75952	1923.8207	802.80702	1951.677	784.93295	1975.4772	737.49311	1927.9861	631.96708	1786.0282	558.8681	1651.8712
187.44571	561.37319	1176.5337	563.04778	1193.1324	545.46699	1204.0435	502.85263	1175.1549	420.619	1084.2989	362.80035	1000.579
334.68417	433.43268	752.17436	432.84663	762.49393	416.85232	766.64421	377.72824	747.39869	308.04671	686.92593	260.95247	632.76753
597.57831	348.93679	463.48009	347.31639	469.52445	333.1877	469.96829	297.18026	457.39034	236.23649	418.17941	196.36481	383.83575
1066.9756	298.16038	291.80276	296.11973	295.37624	283.71851	294.05593	249.5501	285.34669	194.38253	259.36675	158.99463	237.07151
1905.084	264.27752	180.29489	262.11908	182.32511	251.15759	180.20655	218.62219	174.28015	167.65247	157.25739	135.55996	142.98387
3401.526	243.89535	115.9782	241.73403	117.09378	231.7987	115.03443	200.47646	110.67727	152.13042	99.09204	122.037	89.53304
6073.4218	229.47037	75.4552	227.34353	76.13451	218.31087	74.16277	187.87874	70.96323	141.45706	62.82787	112.89491	56.371
10844.09	220.46287	48.59329	217.62871	49.17758	209.42899	47.66461	179.72838	45.25533	134.5933	39.68203	106.95596	35.3628
19362.113	213.12305	33.14432	211.19422	33.70704	202.92183	31.78623	173.68757	29.91938	129.4401	25.84276	102.73521	23.03806
34571.037	207.93857	22.93935	205.80869	23.09726	198.12603	21.50192	169.13741	19.77999	125.959	16.5973	99.73874	14.88439
61726.559	204.29906	18.39621	201.88976	18.79238	194.90198	16.213	165.97489	14.24541	123.44691	11.14388	97.78714	9.73299
110212.72	201.75592	17.80372	199.63594	18.05255	192.6052	14.85226	164.51818	11.47206	121.98715	7.63702	96.64934	5.59049
196784.72	197.78517	19.90043	195.44781	20.30311	189.6395	15.40595	161.92415	10.73706	120.67253	5.49088	95.75612	2.94994
351358.96	192.34657	26.15593	190.52034	26.17724	186.14393	18.56592	160.03968	12.26959	119.76465	4.1573	95.56911	0.67413
627351.13	159.69466	54.49529	157.61486	53.68493	161.20773	42.73044	140.67885	32.9192	107.80252	17.89545	87.09061	10.23722
1120134.9	138.35884	88.92538	134.29119	90.19869	147.05923	68.83179	131.95198	54.06941	104.79073	29.93686	87.10246	16.79309
2000000	90.00055	-0.42723	89.66674	0.49741	101.52474	-7.27793	91.37757	-14.70243	68.90628	-25.83032	56.44603	-29.75168
PEO-LiTFSI@GFC												
0.1	38877.165	127341.39	38573.734	126441.83	37932.713	124753.73	37578.549	121150.29	37074.074	116432.91	36350.043	110450.02

0.17854992	22569.197	79009.572	22290.821	78462.757	21889.964	77596.086	21756.113	75407.239	21367.306	72852.698	21059.133	69239.876
0.31880073	13267.365	48939.293	13156.764	48577.12	12799.945	47988.591	12761.211	46787.041	12481.996	45243.702	12351.238	43239.525
0.56921845	7911.2899	30051.569	7813.2148	29910.252	7643.7722	29510.269	7539.3802	28770.706	7411.2612	27925.073	7257.9976	26722.171
1.0163391	4923.5955	18701.022	4896.6904	18584.246	4759.0506	18311.957	4680.9453	17906.352	4597.8259	17359.647	4470.0851	16684.26
1.8146726	3059.0055	11461.921	3035.9509	11402.482	2952.0799	11215.387	2887.3252	10964.416	2831.3013	10653.206	2754.6432	10286.642
3.2400964	1964.7225	7090.7246	1946.5485	7051.6198	1888.3994	6930.5516	1845.4612	6775.7807	1804.8261	6586.1442	1738.4835	6342.0466
5.7851894	1272.0225	4358.3393	1259.3401	4333.9674	1221.7265	4254.6002	1191.0715	4159.6284	1161.6911	4045.0978	1116.4349	3894.7992
10.329451	856.28735	2685.7228	846.10413	2670.5845	819.99678	2620.4344	798.46579	2562.4247	777.91099	2493.5224	745.32741	2401.1307
18.443226	587.92146	1646.5782	580.01414	1637.2292	560.03926	1606.8937	543.97913	1571.8082	528.88283	1531.2759	504.53687	1476.2246
32.930365	417.49763	999.96212	410.33654	994.47022	393.8907	976.01991	380.87013	955.64016	368.41153	932.34589	348.70544	900.08916
58.79714	318.49222	634.50749	311.82626	631.21045	297.31489	619.51316	285.58552	607.22308	274.52423	593.33069	256.92663	573.58677
104.98225	251.34421	389.12871	244.58425	387.33159	231.76876	380.38395	220.66903	373.41286	210.16703	364.87522	193.53881	353.83295
187.44571	208.33685	237.75729	202.18418	236.51938	189.44403	232.2315	178.91822	228.00957	168.86668	223.46042	153.08535	216.95195
334.68417	183.89086	152.48762	177.82225	151.68247	165.55406	148.86229	155.2538	146.15208	145.39278	143.34432	129.86517	139.33531
597.57831	166.85413	94.71563	160.88079	94.21748	148.98808	92.37341	138.94876	90.62711	129.27033	88.82797	113.99055	86.32501
1066.9756	155.88869	60.53648	149.97665	60.19286	138.37724	58.90336	128.63074	57.70373	119.17174	56.47183	104.14685	54.75761
1905.084	148.05663	38.06333	142.2179	37.84081	130.87855	36.97451	121.37934	36.12732	112.12988	35.26055	97.42501	34.16843
3401.526	143.21755	24.75759	137.42883	24.59839	126.24966	24.00581	116.86273	23.39809	107.79903	22.78207	93.35986	21.97711
6073.4218	139.85722	16.27314	134.1061	16.15029	123.03633	15.7094	113.75632	15.25866	104.80058	14.80772	90.56986	14.22385
10844.09	137.77935	9.98387	132.06656	9.84924	121.11318	9.76149	111.96187	9.30935	103.06098	9.03792	88.81364	8.64418
19362.113	136.50424	6.36379	130.73385	6.29724	119.70971	6.11786	110.60935	5.83614	101.8255	5.82631	87.66855	5.61821
34571.037	135.45309	3.75506	129.83976	3.8155	118.80446	3.57845	109.75253	3.23885	101.09544	3.69869	86.96393	3.37673
61726.559	134.92138	2.5345	129.35987	2.37633	118.32799	2.27221	109.19796	1.97024	100.57097	2.26716	86.48877	1.90569
110212.72	134.39227	2.03602	128.9134	1.66092	118.07897	1.20233	109.04933	0.58021	100.47523	0.42019	86.27141	-0.25145
196784.72	134.06469	1.1545	128.40847	1.18655	117.75123	0.06422	108.77702	-0.77609	100.07392	-1.13997	85.89549	-2.00894
351358.96	133.91059	0.17544	127.74526	-0.2117	117.73669	-1.18677	108.6669	-2.57433	100.5568	-3.35549	86.35861	-5.0934
627351.13	121.43458	14.82221	116.18124	14.09717	106.83747	11.45433	99.71247	8.48679	91.81685	6.39666	80.07768	2.2929
1120134.9	120.88326	26.67676	115.72473	22.59115	110.68698	17.81928	101.2175	14.88365	94.41535	10.08181	83.82814	4.21005
2000000	81.10572	-32.02334	76.80512	-36.57044	69.17469	-34.51329	67.33604	-40.60341	57.10533	-37.05468	47.65924	-41.0179
PEO-LiTFSI-LLZTO@GFC												
0.1	54993.742	149523.59	54609.383	146348.74	53807.478	141657.73	51973.716	135208.61	50085.141	125829.94	47766.34	117032.44
0.17854992	34263.204	95270.211	33792.231	93238.135	33141.483	90611.689	32096.406	86403.753	30718.16	81057.882	29545.829	75527.601
0.31880073	20905.114	60460.431	20688.543	59563.962	20316.936	57946.748	19868.381	55444.586	19012.436	51946.471	18316.87	48783.809
0.56921845	12992.806	38368.828	12901.169	37768.52	12689.269	36798.76	12367.405	35179.581	11916.297	33137.994	11481.315	31149.575
1.0163391	8298.8094	24541.021	8196.3855	24166.852	8067.3485	23575.464	7871.2413	22638.146	7590.3597	21335.225	7326.7485	20136.654
1.8146726	5171.6903	15524.388	5125.5769	15300.7	5049.574	14939.706	4928.755	14358.907	4769.7743	13582.222	4604.7149	12837.286
3.2400964	3253.9081	9875.4918	3229.1231	9739.825	3186.2372	9525.614	3115.3304	9169.9836	3017.794	8699.4444	2921.4074	8246.3156

5.7851894	2023.5869	6215.4754	2010.6484	6135.3713	1983.9198	6005.9134	1942.6033	5795.9436	1883.3642	5515.2794	1827.0506	5241.4248
10.329451	1288.1499	3900.7066	1280.0088	3853.0982	1262.759	3776.4674	1235.6553	3652.7015	1196.561	3485.9122	1160.7531	3322.2311
18.443226	825.39425	2426.7494	819.95832	2399.9317	807.12301	2354.7384	788.42068	2281.97	760.2609	2183.0838	736.43022	2086.863
32.930365	536.3114	1495.0134	532.23834	1478.9674	522.89167	1452.6616	508.3408	1409.9676	486.74105	1351.6873	469.56543	1295.4562
58.79714	368.17673	958.96892	365.069	949.19724	357.28692	932.8168	345.7916	906.74958	328.7649	870.40939	315.14742	835.94601
104.98225	254.48544	594.69688	251.86396	588.90729	244.96096	579.74501	236.0236	563.37474	222.0073	541.62181	210.52345	521.61912
187.44571	181.4662	365.38462	179.39784	362.14682	173.99986	356.45929	165.7257	347.2651	153.63119	334.5255	144.3658	322.50438
334.68417	140.87293	233.99104	138.94287	232.12216	133.87637	228.712	126.30554	223.15809	115.07904	215.47297	106.66827	208.21376
597.57831	114.08618	143.54531	112.20485	142.46326	107.33146	140.53738	99.99243	137.41329	89.206	133.06413	81.19307	128.94597
1066.9756	98.60116	89.31499	96.74733	88.68209	91.93859	87.53888	84.71451	85.7004	74.0802	83.12484	66.19489	80.83129
1905.084	88.89061	54.13721	87.09082	53.79028	82.35798	53.10897	75.21602	51.98889	64.70515	50.45078	56.88819	49.06356
3401.526	83.46725	33.81944	81.69282	33.60966	77.02326	33.17227	69.93928	32.46375	59.5368	31.468	51.79952	30.60377
6073.4218	79.93153	21.10096	78.17437	20.96807	73.55808	20.67082	66.5433	20.20626	56.24744	19.52888	48.60161	18.9276
10844.09	77.88726	12.74332	76.12477	12.64744	71.538	12.45294	64.56742	12.19626	54.3537	11.76055	46.75395	11.3565
19362.113	76.56054	7.90507	74.84571	7.85669	70.25108	7.68392	63.27836	7.46716	53.1298	7.1734	45.58728	6.80442
34571.037	75.74497	4.71848	73.99893	4.60713	69.42165	4.53539	62.52342	4.334	52.38045	4.03488	44.87708	3.70739
61726.559	75.19211	2.60359	73.48282	2.59242	68.92891	2.41752	62.06346	2.18723	51.94567	1.88728	44.45016	1.42019
110212.72	74.9918	0.42639	73.20115	0.346	68.77595	0.14519	61.91716	-0.06261	51.81957	-0.39025	44.30489	-1.07806
196784.72	75.07559	-1.42684	73.4042	-1.51936	68.89408	-1.88133	61.93775	-2.26401	51.88164	-2.80039	44.38489	-3.07982
351358.96	74.98119	-3.73122	73.24907	-3.94113	68.73883	-4.51039	62.04716	-5.23971	52.05209	-6.07348	44.45161	-6.57156
627351.13	69.05116	2.6081	67.87528	2.21322	64.08314	1.10149	58.26486	-1.00234	49.38057	-3.32182	42.55686	-5.19731
1120134.9	70.25733	3.00253	69.46569	2.63153	65.59095	-0.21034	60.33107	-2.60562	52.17057	-7.06277	45.60231	-10.02438
2000000	39.42382	-33.79511	38.01575	-33.62524	36.23895	-33.93553	32.2787	-35.16902	25.71562	-36.5834	20.33502	-35.81561

Table S3 Benckmark of GFC and LLZO-based filler CPEs.

M_{PEO} (g/ mol)	Filler type	[EO]:[Li^+]	Ionic conductivity ($S\ cm^{-1}$)	t_{Li^+}	ESW (V)	Reference
600,000	Without filler	18:1	7.9×10^{-6} at 30°C	0.24	4.2	S1
	GFC		1.1×10^{-5} at 30°C	0.3	5.2	
600,000	20 wt% LLZTO (8.7 μm)	18:1	7.49×10^{-5} at 70°C	-	4.75	S2
	40 wt% LLZTO (8.7 μm)		1.00×10^{-3} at 70°C	-	5.5	
600,000	10 wt% LLZTO (0.5 μm)	12:1	6.77×10^{-5} at 30°C	0.117	4.5	S3
	40 wt% LLZTO		3.5×10^{-5} at 30 °C	0.101	4.8	

	(0.5 μm)					
600,000	50 wt% LLZTO	15:1	2.12×10^{-4} at 60°C	-	4.5	S4
600,000	50% LLZTO	10:1	3.31×10^{-4} at 60°C	-	5.2	S5
600,000	Without filler	10:1	9.47×10^{-5} at 27°C	0.106	4.0	This work
			2.00×10^{-4} at 50°C			
	15 wt% LLZTO (5~8μm) and GFC		3.00×10^{-4} at 27°C	0.266	4.9	
			4.90×10^{-4} at 50°C			

Reference

S1. Z. Zhang, Y. Huang, H. Gao, C. Li, J. Huang and P. Liu, *Journal of Membrane Science*, 2021, **621**.

S2. C.-Z. Zhao, X.-Q. Zhang, X.-B. Cheng, R. Zhang, R. Xu, P.-Y. Chen, H.-J. Peng, J.-Q. Huang and Q. Zhang, *Proceedings of the National Academy of Sciences*, 2017, **114**, 11069-11074.

S3. H. Zhuang, W. Ma, J. Xie, X. Liu, B. Li, Y. Jiang, S. Huang, Z. Chen and B. Zhao, *Journal of Alloys and Compounds*, 2021, **860**, 157915.

S4. L. Zhang, J. Feng, G. Zhu, J. Yan, S. Bartlett, Z. Wang, Z. Hao, Z. Gao and R. Wang, *ACS Applied Materials & Interfaces*, 2024, **16**, 13786-13794.

S5. Z. Huang, R.-a. Tong, J. Zhang, L. Chen and C.-A. Wang, *Journal of Power Sources*, 2020, **451**, 227797.